Int. J. Electrochem. Sci., 12 **(2017)** 11122 – 11136, doi: 10.20964/2017.12.53

International Journal of ELECTROCHEMICAL SCIENCE
www.electrochemsci.org

Biodegradable Polylactic acid and Polylactic acid/Hydroxyapatite Coated Iron Foams for Bone Replacement Materials

Monika Hrubovčáková[*], *Miriam Kupková, Miroslav Džupon, Mária Giretová, Ľubomír Medvecký, Róbert Džunda*

Institute of Materials Research, Slovak Academy of Science, Watsonova 47, SK-04001 Košice, Slovak republic
[*]E-mail: mhrubovcakova@saske.sk

Received: 3 August 2017 / *Accepted:* 21 September 2017 / *Published:* 12 November 2017

Biodegradable iron open cell foams fabricated via replica method have been studied as a potential material for bone scaffold. In order to improve their degradable behaviour and biocompatibility, the polylactic acid and polylactic acid/hydroxyapatite coatings were applied on foams. Microstructure of uncoated and coated iron foams was investigated using scanning electron microscopy. In vitro degradability of the manufactured foams was tested using electrochemical and static immersion tests in a simulated body fluid - Hank's solution. Mechanical properties and biocompatibility were studied by compression test and cytotoxicity test. The manufactured cellular foams have exhibited a highly porous 3D structure with open interconnected macropores similar to that of a cancellous bone. The presence of coatings on the foams' struts improved their mechanical properties and accelerated their biodegradability as compared to uncoated ones. Cytotoxicity test revealed that the presence of polylactic acid and polylactic acid/hydroxyapatite coating increased the cell viability.

Keywords: biodegradable metals, bone scaffolds, iron foams, biodegradation, mechanical properties

1. INTRODUCTION

The bone has a composite nature, containing both organic and inorganic components with a highly organized hierarchal structure. A unique feature of the bone is its ability to remodel itself to repair smaller damage [1]. Notwithstanding, when bone defects caused by diseases or injury exceed the limits of the bone's ability to self-repair, an external intervention is required.

Metallic biodegradable materials have been intensively investigated as a potential material for temporary medical implants in osteosynthesis and cardiovascular surgery [2-15]. Degradable metals

exhibit better mechanical properties for load-bearing than polymers [10]. At the beginning of the healing process, the temporary devices carry the full load. As the healing process progresses, the implant is gradually dissolved, absorbed and excreted without forming toxic products. The load-bearing activity is gradually transferred to the newly regenerated bone tissue [2]. Degradable devices may solve disadvantages of permanent implants such as chronic inflammation or a prolonged physical interaction [11].

Several recent studies have shown that iron and its alloys are perspective biodegradable metals for temporary devices, especially for load-bearing implants, because of their good mechanical properties [2], biocompatibility and nontoxic nature [5].

Porous metals are especially promising as bone scaffolds, because in addition to the reduction of stress shielding, they also allow for the ingrowth of the new bone tissue and the exchange of the body fluids [16, 17], thus contributing to bone reparation. Optimal regeneration requires that the implanted scaffold material meet certain morphological and mechanical criteria [17, 18]. An ideal bone scaffold should resemble the structure and mechanical properties of the natural bone [18].

Biodegradable iron foams are the most promising in this regard, but the literature offers little information on their use in tissue scaffolding. Only a handful of studies have focused on their biocompatibility, degradation rate improvement, and mechanical properties [18-25].

At the same time, however, the use of iron-based implants is somewhat challenging in that their degradation is considered too slow [5]. Several approaches have been suggested to accelerate the rate of iron corrosion, such as alloying [2, 7, 11, 12], introducing new fabrication methods [8], and surface modification [9]. A new method of stimulating iron degradation is environment acidification [22]. This in turn facilitates the solubility of the dense degradation products of iron, such as iron hydroxides, phosphates and carbonate, because these inhibit further corrosion [26, 27]. This method is grounded in the fact that polymers degrade via hydrolysis, whose degradation rate escalates with acidity. Yusop et al. [22] proposed that the presence of polymers on the iron surface contributes to the acidification of the surrounding environment and as such could increase the solubility of the corrosion products.

The crucial task in the research of current bone implants is to increase the bioactivity of the biomaterial and ameliorate the interfacial biocompatibility [28, 29]. In vitro cytotoxicity tests of porous Fe, Fe-Mg, Fe-Mg and Fe-CNTs showed that the product of Fe degradation was nontoxic to endothelial cells [30], but low proliferation of osteoblasts was observed [20].

Many studies have been carried out with the objective of improving the coating quality and optimizing the modifications of metal surfaces [31,32]. Hydroxypatite (HAp) is a well-known bioactive ceramics. HAp coatings are very often applied to bio-inert ceramic or metallic implants to support the healing process of hard tissues [33,34,35], because they support cell proliferation, osteointegration and tissue ingrowth. However, HAp alone is brittle. To overcome this problem, the use of HAp composites with degradable polymers have been proposed [36]. Polymers combined with calcium phosphate not only partially solve the brittleness, but also promote the osteoblasts' adhesion, migration, differentiation and proliferation, so these composite materials have the potential to be used in bone repair and regeneration. Not only does the polymer component improve adhesion to the substrate, but can also act as a vehicle for biomolecules and antibiotics [37]. Degradable organic polymers such as

polycaprolactome (PCL), polylactic acid (PLA) and polylactic glycolyc acid (PLGA) are usually used for this purpose [38,39].

Another advantage of applying composite polymer ceramic coating is achieving better mechanical properties, especially in case of highly porous materials.

The objective of the present work is using sintered iron foams produced via replica method as biodegradable materials. To accelerate their corrosion rate and improve biocompatibility and mechanical properties, the iron foams were coated with polyme r- polylactic acid and composite polylactic acid/hydroxyapatite coatings. The prepared foams were tested for their microstructure, degradability, mechanical properties and biocompatibility.

2. EXPERIMENTAL

2.1 Materials preparation

Iron scaffolds with interconnected porous structure were produced via replica method. Polyurethane (PU) foam, Bulpren S (POLY Slovakia) with cell 50-65 PPI size, was used as a sacrificial template. The foam specimens of (15x20x5 mm) were infiltrated with slurry prepared from distilled water, 5 wt.% polyvinyl alcohol solution (Sigma Aldrich) and commercially available carbonyl iron (type CC, d50 3.8-5.3μm, BASF, Germany). The infiltration of PU foam with a suspension containing iron particles for 3min was repeated twice. The superfluous slurry was removed by rolling. Impregnated foam specimens were dried and thermally treated using a 2-stage protocol. The specimens were annealed at 450°C for 2h in pure N_2 atmosphere to decompose the organic template. Subsequently, the metal structures were sintered at 1120°C for 1 h in atmosphere of 10%H_2-N_2. The preparation method was in detail described in our previously work [25].

The manufactured iron scaffolds were coated with polymer polylactic acid (PLA) and composite polylactic acid/hydroxyapatite (PLA/HAp) coatings, respectively. PLA granules supplied by Sigma Aldrich were dissolved in chloroform at room temperature and homogenously stirred for 48 hours to produce a solution of 5wt.%. To produce a PLA/HAp solution, PLA pellets and HAp powder prepared according to [40] in ratio 1:1 were dissolved in chloroform (5% weight/volume ratio) at room temperature and stirred for 48 hour. In both cases, solutions were stirred under reflux. The iron scaffolds were ultrasonically cleaned in acetone and ethanol and then dried. The samples were coated in five cycles with a constant down and withdrawal speed of 200 mm/min, using a dip coating machine. The scaffolds with both PLA and PLA/HAp coating, respectively, were dried at room temperature for 48 hours.

2.2 Materials characterization

The microstructure and surface morphology of manufactured metallic foams, both uncoated and coated, were examined by scanning electron microscope (Jeol JSM 7000F, Japan), equipped with energy-dispersive analyzer INCA EDX. Before SEM observation, the coated samples were sputter-

coated with a thin layer of gold. The sintered densities and porosity were calculated by the Archimedes principle [25].

2.3 The degradation tests

The degradation behaviour of thus produced uncoated and coated iron foams was studied by static immersion test and electrochemically by potentiodynamic polarization.

The electrochemical corrosion behaviour was tested using the potentiostat PARSTAT 4000 (Princeton Applied Research, USA) interfaced to a computer. The tests were carried out in a simulated body fluid (SBF) – Hank's solution at a constant temperature of 37±0.5°C. Hank's solution with pH value of 7.4, was prepared from distilled water and chemicals of laboratory grade; its composition was as follows: 8 NaCl, 1.00 glucose, 0.4 KCl, 0.06 $NaH_2PO_4 \cdot 2H_2O$, 0.14 $CaCl_2$, 0.06 $MgSO_4 \cdot 7H_2O$, 0.35 $NaHCO_3$, 0.60 KH_2PO_4 and 0.10 $MgCl_2 \cdot 6H_2O$ (in g/l). A three-electrode cell was used, where a foam specimen served as the working electrode, a saturated calomel electrode as the reference electrode and a platinum foil as the countered electrode. We tested three specimens of each scaffold type. The working electrode with an exposed area of about 0.5 cm^2 was initially immersed in the electrolyte for 7200s to measure Open Circuit Potential (OCP). After stabilization, the potentiodynamic polarization was recorded by varying the potential from -250 mV to +250 mV relative to OCP at a scanning rate of 0.1666 mV/s. The electrochemical parameters: corrosion potential E_{cor}, corrosion current densities (i_{corr}) and corrosion rate *(CR)* were determined using software VersaStudio according to Tafel extrapolation.

In vitro degradation behaviour of specimens was also studied by a static immersion test. Experimental specimens were initially ultrasonically cleaned in distilled water and ethanol (each for 10 minutes). The specimens were dried, weighed and subsequently immersed in 50 ml of Hank's solution and incubated for 8 weeks at 37±0.5°C. The corroded foams were removed from SBF after every 7 days of immersion. To remove degradation products, samples were ultrasonically purified in distilled water and ethanol, each for l0 minutes and then dried at 80°C for two hours, and subsequently weighed.

2.4 Mechanical tests

We performed mechanical tests of uncoated and coated iron foam scaffolds at room temperature under uniaxial compression. The test were done by universal testing mashing (TiraTest 2300, GERMANY), at a head speed of 0.001mm/s and load of 1kN. Five samples of each experimental group with dimensions of 15x12x5mm were tested. The yield strength and elastic modulus were determined by ASTN D1621-00 and ISO 844 standard. The offset yield strengths were determined as stress values at 0.2% plastic strain.

2.5 Cytotoxicity test

MC3T3E1 mouse pre-osteoblastic cells (ECACC, Salisbury, UK) in subconfluency were harvested from culture flasks by enzymatic digestion (trypsin-EDTA solution). The cells were suspended in a culture medium and the cell suspension was adjusted to a density of $125x10^3$ cells/ml. Uncoated samples and samples with polymeric coating were sterilized under UV light in a laminar flow hood, each side of the samples for 30 minutes. The samples (3 samples for each well) were placed at the bottom of the wells of a 48-well microplate (not cell culture-treated) and 5×10^4 of MC3T3E1 cells were seeded onto sample surface in each well in 400 µL of Minimum Essential Medium Eagle (EMEM) with 10% FBS and 1% ATB-antimycotic solution (Sigma-Aldrich). The culture plate was cultivated in an incubator at 37°C, 95% humidity and 5% CO_2. After 4, 24 and 48 hours of cultivation, the density, distribution and morphology of the MC3T3E1 cells were evaluated on the tested samples using a fluorescence optical microscopy (Leica) with the live/dead staining based on fluorescein diacetate (FDA)/propidium iodide (PI). Unlike the PI, which passes only through the damaged membranes of dead cells and stains the cells red, the FDA is converted to a green fluorescent product upon hydrolysis by intracellular esterase's of living cells.

3. RESULT AND DISCUSSION

3.1 Scaffold characterization.

The structure of metallic foams - porosity, pore size, pore distribution and interconnectivity, are the key factors, which significantly affect the biological performance and the mechanical properties of a bone scaffold [41].

Fig.1 presents SEM surface morphology of an iron foam fabricated by replica method before and after coating with PLA and PLA/HAp. As can be seen, the uncoated foams, Fig. 1a, exhibited an open, highly porous structure of interconnected macropores. The interconnected network of macropores not only affected the level of penetration and tissue ingrowth, but also the transportation of nutrients and metabolic waste into and out of the scaffold [41]. Bone reparation generally requires the pore size range of 100-500µm to allow the ingrowth of the vascular tissue [42]. However, large pores are an advantage in case of larger implants, because they allow a deeper penetration of the host tissue [24]. The pore size of the manufactured foams ranges between 300 and 800 µm. The pores were evenly distributed and had the same size. A large amount of small pores is visible on the surface of the macropores' struts. These micropores, formed during sintering, are beneficial to scaffold stabilization and may enhance conductivity. Similar morphological structure of metallic scaffold manufactured via replica method was already reported [24, 43]. Replica method allows for the preparation of metallic foams with an open, three-dimensional interconnected macroporous structure similar to that of a cancellous bone [43]. This method gives us the advantage of measuring the foam's pore size by choosing the right default template.

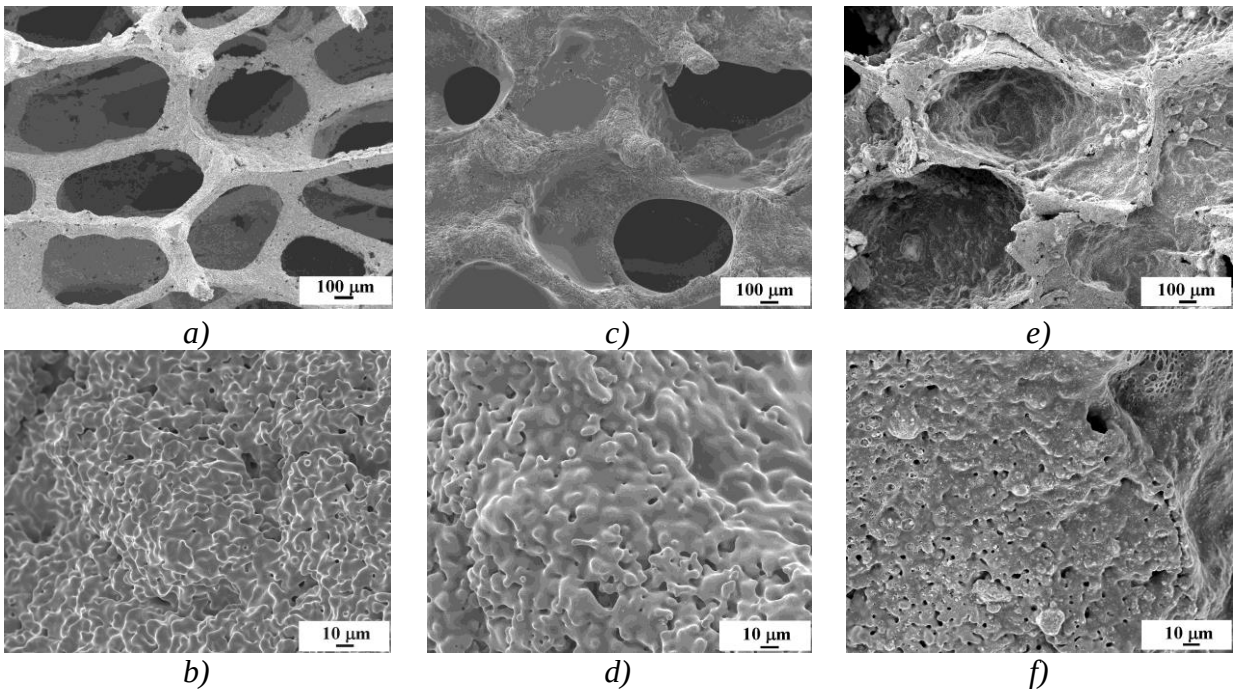

Figure 1. SEM images of surface morphology of:a-b uncoated, c-d PLA, e-f PLA/HAp coated iron foams, prepared by replica method.

After coating, the structure of the experimental foams remains unchanged. Both PLA and PLA/HAPp coatings homogeneously cover the surfaces of iron struts. As can be seen, Fig.1d, f, the micropores on the strut surfaces are partially filled with coatings, which may have positively affected the mechanical properties of scaffold. The surface of PLA/HAp coated specimens was always rougher in comparison to those coated with PLA. Hydroxyapatite is homogenously dissolved in PLA matrix, agglomerates are visible only rarely. It should be noted that characteristics of the coatings were not studied in detail in this work.

The total porosity of the uncoated iron scaffold ranged from 89 to 93%. After applying PLA and PLA/HAp coating, Fig. 1c, e, the pores were partially closed due to the formation of coating films bridging the cell walls, which affected the porosity of the coated foams. The total porosity of the coated iron scaffolds decreased. In case of PLA coated foams, we attested a decrease to 83-89%, for those coated with composite PLA/Hap, it was 80-85%. Similar results were arrived at in the work of Stipniece et al. [44], who studied TiO2 scaffolds coated with polyvinyl alcohol and hydroxyapatite/polyvinyl alcohol.

3.2 Corrosion behaviour.

3.2.1 Electrochemical behavior

Scaffold degradation is an important parameter for bone regeneration, because appropriate scaffold degradation provides the space for the matrix deposition and tissue growth, which may ultimately improve the quantity and quality of the regenerated bone [45].

We carried out electrochemical studies of corrosion behavior, including the open circuit potential (OCP) versus time and potentiodynamic polarization. Potentiodynamic polarization curves were measured after stabilization (7200 s). Fig.2 presents the typical potentiodynamic polarization curves of the uncoated iron foams and those with PLA and a PLA/HAp coating.

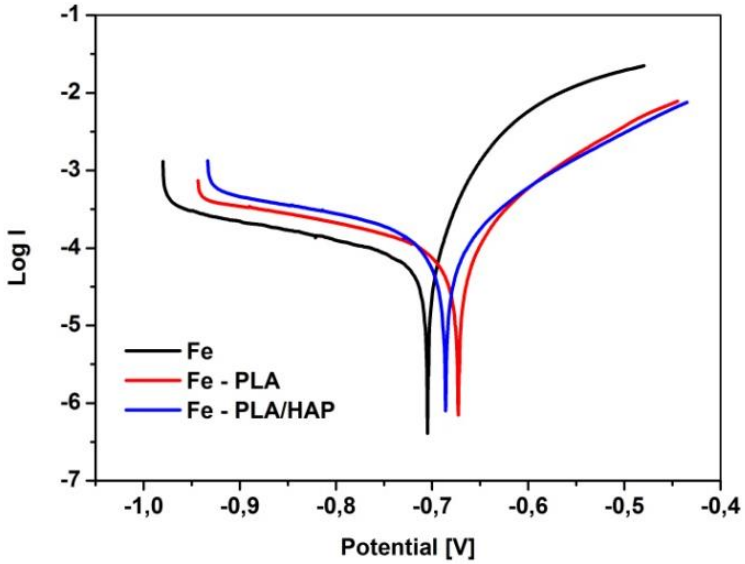

Figure 2. Potentiodynamic polarization curves of uncoated and PLA and PLA/HAp coated iron foams, prepared via replica method, in Hank's solution at pH 7.4 and 37±0.5°C at scan rate 0.1666 mV/s.

The average values of corrosion characteristics, corrosion potentials (E_{corr}), corrosion current densities (i_{corr}), corrosion rate *(CR)* and anodic and cathodic Tafel slops (b_a, b_c) are summarized in Table 1.

Table 1. The average values for the corrosion potentials (E_{corr}), corrosion current densities (i_{corr}) and the corrosion rate (CR) and anodic and cathodic Tafel slops (b_a, b_c) of the manufactured foams obtained from the potentiodynamic polarization curves in Hank's solution at pH 7.4 and 37°±0.5C.

SAMPLE	E_{CORR} [mV]	i_{CORR} [μA/cm^2]	*CR* [mm/y]	b_a [mV/dec]	b_c [mV/dec]
Fe	-704.6	26.68	0.31	412.7	43.7
Fe-PLA	-672.6	66.12	0.65	551.3	162.9
Fe-PLA/HAp	-685.7	41.63	0.48	468.1	106.1

The corrosion potential for the coated foam samples was shifted to more positive values as compared to the uncoated ones. It indicates that the coating layer is more noble at the early stage and needs more energy to initiate the corrosion reaction. The corrosion rate is kinetically measured by the corrosion current densities*(i_{corr})*, where a lower value of i_{corr} represents a lower corrosion rate [46].

The corrosion current density of the tested foams decreases according to the sequence Fe-PLA>Fe-PLA/HAp>Fe. As can be seen in Table 1, the coated foams had higher corrosion rates than the uncoated, i.e. 0.31, 0.48 and 0.64 mm/y, for Fe, Fe-PLA/HAp and Fe-PLA foams, respectively. This indicates that the degradation of the iron foams was accelerated in the presence of PLA. This is in accordance with Yusop et al.[22] who reported that PLGA (poly-lactic-co-glycolic) infiltrated iron foams degraded faster than the ones made of pure iron. PLA degrades via hydrolysis in physiological environment and comes along with an increase in local acidity [47]. It may increase the solubility of iron degradable products [22]. The degradation of the PLA/HAp coated iron foams was lower in comparison to the PLA coated ones. The corrosion inhibition effect of hydroxyapatite in composite coating has already been reported [48]. This is caused by the accumulation of phosphate product from Hank's solution and from HAp. Such finding is consistent with a previous study by Xu et al. [49] who studied corrosion inhibition of magnesium alloy by phosphating treatment. The decrease in the degradation rate of magnesium alloy due to HAp presence was also reported by Dieringa et al. [50] and by Jamesh et al. [51]. Similar results were also arrived at by Orinakova et. al. [48] who studied biodegradable iron materials with a bioceramic HAp coating.

3.2.2. Static immersion behavior

Degradation of the manufactured foam specimens was evaluated by the mass loss measurement in Hank's solution at 37±0.5°C for 8 weeks.

Fig.3 shows a mass loss of foam specimens after an immersion test over a different time period. A significant mass loss of uncoated iron and PLA/HAp coated foams was observed after 3 weeks of immersion, while the PLA coated foams degraded gradually. After 8 weeks, the mass loss of individual experimental specimens was as follows: Fe<Fe-PLA/HAp<Fe-PLA. The results correspond to electrochemical corrosion measurements.

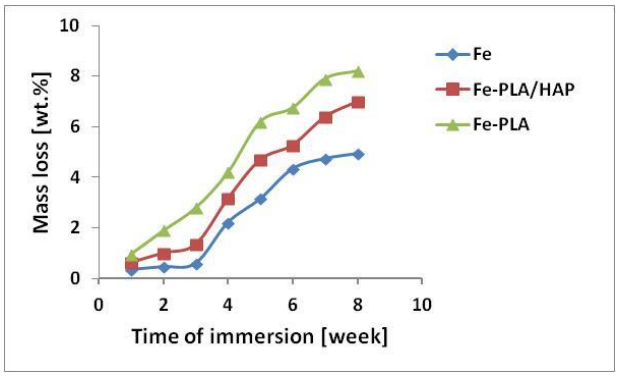

Figure 3. The mass loss of the uncoated and PLA, PLA/HAp coated iron foams in Hank's solution at 37±0.5°C for 8 weeks

Fig.4 shows SEM micrographs of the surface morphology of the experimental foams after 8 weeks of degradation. The struts of all experimental foams were covered with a brownish layer of corrosion products. After 8 weeks of immersion, the residual polymer coating was still present on the struts of the PLA coated foams. The incorporation of the inorganic phase (HAp) to a PLA matrix reduced the degradation of the PLA/HAp coated foams. There were visible residues of HAp agglomerate on the struts surface of PLA/HAp coated foams, indicating that the organic phase of the composite PLA/HAp coatings dissolved first. Big pits and cracks were observed on the surface of all experimental specimens.

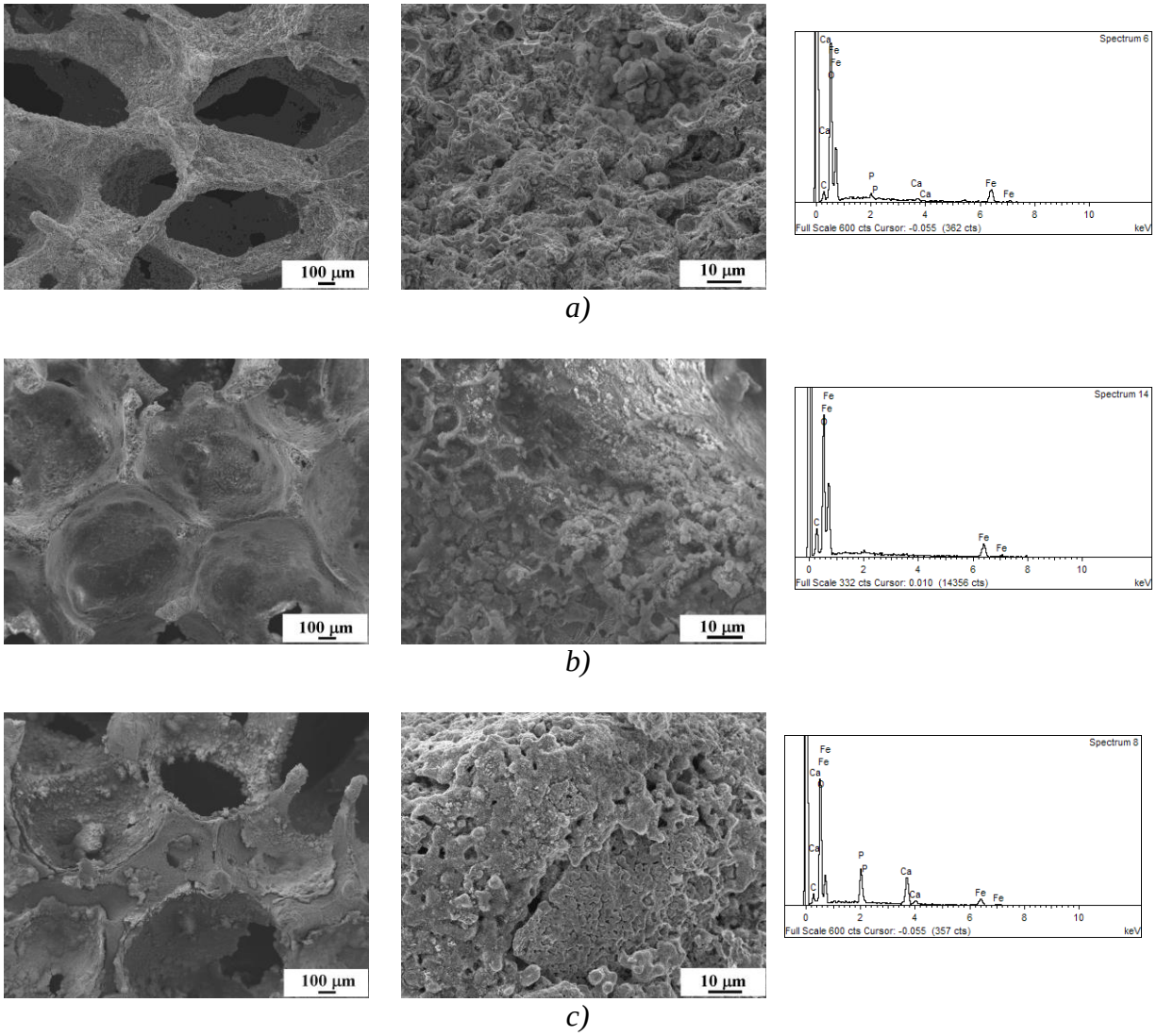

Figure 4. SEM image and EDX analyses of a) uncoated and b) PLA and c) PLA/HAp coated iron foams after an 8 week long immersion test in Hank's solution at 37±0.5°C.

EDX analyses of the degraded products of the uncoated and PLA/HAp coated foams, Fig.4, confirmed the presence of a phosphate product from physiological solution and HAp coating. The presence of Ca and P ions in the corrosion layer of the PLA coated foams was not confirmed. PLA

degrades into a water soluble monomer - lactic acid- with a carboxylic end group; this process is associated with pH decrease [47]. The acidic environment is known to accelerate the solubility and dissolution of iron degradation products [22]. The heterolytic cleavage of O-H bond of a carboxylic acid is bound with H^+ ions formation. These can form hydrogen after reacting with the electrons at iron surface. The hydrogen formation disturbs the created corrosion layer and thus facilitates the oxygen diffusion on the iron surface and accelerates degradation [22].

3.3 Mechanical properties

The response of open-cell foams to compression is universal, regardless of the makeup of the foam. The stress-strain curve usually has three characteristic regions: 1) small compressive strains constituting a quasi-elastic linear increment of the stress value, 2) followed by a "plateau" region with no or negligible slope of the curve, 3) and region of densification, where the stress increases rapidly [51]. The initial linear response of the foam (the elastic deformation) to an increase in stress is determined by the cell edges and their faces which bend and stretch. The subsequent collapse of cells is responsible for the plateau region of the stress-strain curve. Depending on the material of the foam in question, the collapse can be caused by either brittle crushing or plastic yielding of cell edges and faces. For example, the plateau of the stress-strain curve is usually rather notched in case of brittle skeletons but quite smooth in case of a solid ductile skeleton. The slope of this region is determined by the type of cells – to be more precise, whether they are open or closed. As a rule, open-cell materials have a long, flat plateau, because the load required for the collapse is almost constant. On the contrary, deformation of closed-cell materials requires continuous increments of the compression load. This is caused by the gas entrapped inside the cells and higher rigidity of the cell walls; both variables resist the compressive stress.

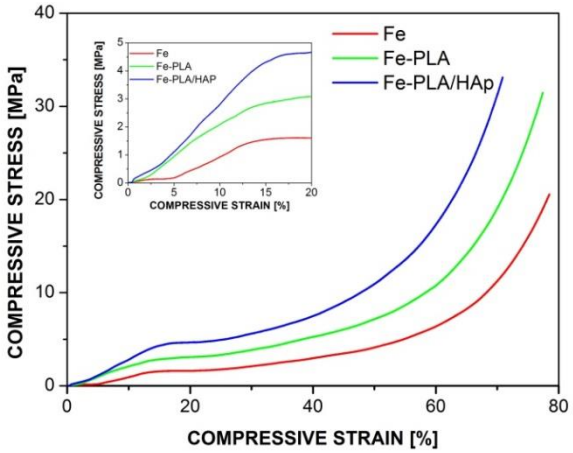

Figure 5. Compressive stress-strain curves of uncoated, PLA and PLA/HAp coated iron foams manufactured by replica method

Apart from that, there is an inverse variation between the foam density and the length of the plateau region universal to all foams [51]. As the compression stress increases further, foams become densified. The faces and edges of their cells get in contact, transforming a porous material into a virtually solid material. This explains a rapid stress increase in the final region of the stress-strain curve.

Typical compressive stress-strain curves for uncoated and PLA and PLA/HAp coated iron foams are shown in Fig.5. All of them display the quasi-elastic deformation, which is later followed by a plastic deformation. In addition, they come with a smooth and regular plateau region, a feature typical of ductile metallic foams. The region where elastic deformation occurs is within 3% to 10% of strain in all specimens. Such a narrow range suggests a low elastic deformation of the foams taking place at low compressive stress which afterwards turns into a large plastic deformation. The yield stress was defined as the stress necessary for a plastic deformation of 0.2%. The compressive strength of all available foams is within 0.2-10 MPa, like that of a cancellous bone [52 ,53]. Yusop et al. [22] reported similar results for iron foams infiltrated by biodegradable polymers poly(lactic-co-glycolic acid). When compared to a pure iron foam sample, the presence of coatings enhanced the yield strength for both PLA and PLA/HAp coated foams, Table 2. The mechanical properties of metal foams are influenced by numerous factors, e.g. pore size, porosities, densities and the properties of the parent material [18]. The PLA and PLA/HAp coatings fill in the micropores and other crack defects on the struts, thus causing the total porosity to decrease. This has a significant impact on the mechanical strength of the experimental foams. The samples with the highest yield strength and elastic modulus turned out to be those with Fe-PLA/HAp coating.

Table 2. Mechanical properties of uncoated and PLA and PLA/HAp coated iron foams.

Samples	Yield strength [MPa]	Elastic modulus [MPa]
Fe	1.3 ± 0.18	15.2 ± 0.63
Fe-PLA	2.5 ± 0.35	21.2 ± 3.58
Fe-PLA/HAp	4.0 ± 0.21	34.5 ± 1.61

The improvement of mechanical properties by poly-(D,L-lactic acid) coatings of ceramic TiO2 scaffold have been previously reported by Novak et.al [54] and by Stipniece et.al. [44] who studied hydroxyapatite/poly vinyl alcohol coated porous TiO2.

3.4 Cytotoxicity test

Cell attachment, migration, and poliferation in the porous structure are important cell-material interaction parameters that determine its suitability in scaffold use [23]. Osteointegration can be

improved by applying bioactive coatings, e.g. hydroxyapatite, a well-known bioactive material. Using HAp coatings on metallic implant has proved to stimulate a faster cell attachment, which resulted in an improved healing rate during the early implantation stage [55, 56]. The micrographs of the initial cell attachment of osteoblasts (live/dead staining), Fig. 6, demonstrate that after 4 h from seeding, the cells well adhered to substrates, but the cell density was lower when compared to a standard titanium surface. Similarly, most cells were insufficiently spread on samples and had more spherical shape.

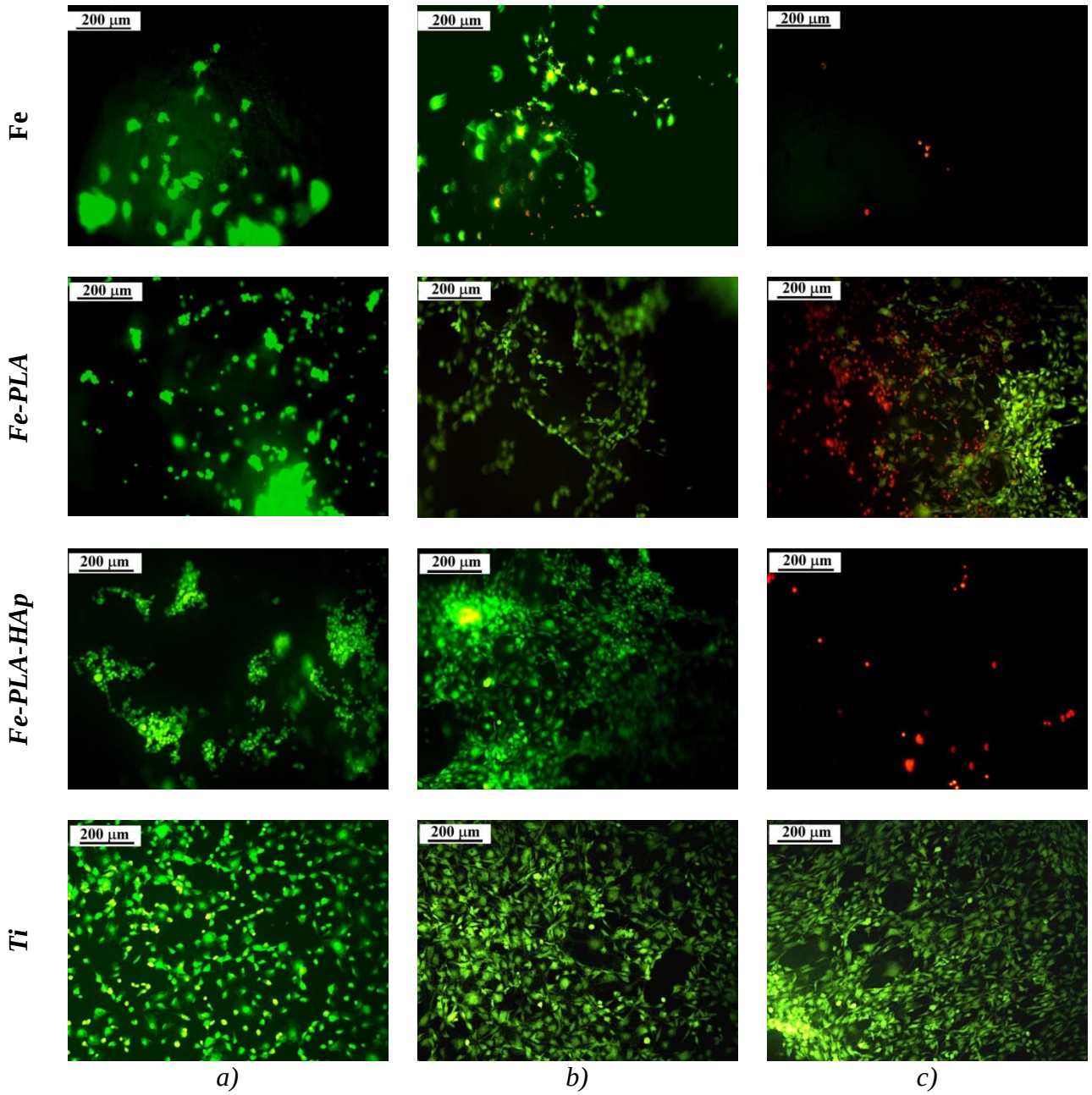

Figure 6. Fluorescent micrographs of osteoblasts on the surface of uncoated and PLA, PLA/HAp coated iron foams and Ti standard after a) 4hours, b) 24 hours and c) 48 hours adherence.

The dense coating of cells was measured on Fe-PLA/Hap sample, wherein the cells were deposited on the pore surface. After 24 hours of cultivation, the osteoblasts were spread much better, although we found some fractions of dead cells (red colored) on Fe and Fe-PLA/HAP substrates, which proves increased cytotoxicity in samples with a prolonged cultivation.

Almost the same cell density was found on Fe-PLA/HAP and titanium, which resulted from a non-cytotoxic character of the samples' surface after 24 hours of cultivation. Completely different images were captured after 48 hours of cultivation. No live cells were identified on Fe and Fe-PLA/HAP samples; a high fraction of dead cells, clearly separated from the fraction of live cells, was visible on Fe-PLA and a low density of live cells was found on Fe-PLA/HAP. Note that a more accurate statistical evaluation of live/dead cell fractions was not possible due to weak adherence of osteoblasts (especially dead osteoblasts) to sample surfaces. The samples were not thoroughly washed before staining to avoid washing away of the dead cells.

Polylactic acid combined with hydroxyapatite ameliorated the interfacial biocompatibility and increased bioactivity of iron biomaterial [57, 58]. Not only did the composite coating of polymers and calcium phosphate improve bioactivity, but also enhanced osteoblast adhesion, migration, differentiation and proliferation [21].

4. CONCLUSION

In this study, porous iron foams with an open interconnected structure, similar to that of a cancellous bone, were successfully manufactured via replica method. The pore size ranged between 300 to 800 μm, and porosity was above 90%. To improve biocompatibility and accelerate their degradability, PLA and PLA/HAp coatings were applied. Both electrochemical and static immersion test showed that coated foams degraded faster than the uncoated ones. The highest corrosion rate was observed for the PLA coated iron foams. This indicates that the PLA hydrolysis accelerated degradation. On the other hand, the presence of HAp in composite coatings slowed it down. The presence of coatings improved the mechanical strength of the coated foams as compared to the uncoated ones. PLA and PLA/HAp coated specimens exhibited better mechanical properties than uncoated samples. Osteoblasts were found to maintain higher viability when in contact with the coated samples, thus indicating a positive effect of HAp cytocompatibility improvement. Iron foams prepared via powder metallurgy replication route with PLA and PLA/HAp coatings seem to make for a good biodegradable bone scaffold material capable of bearing high loads. Nevertheless, further research of the in vitro biocompatibility and the regulation of biocorrosion rate of such materials will be needed.

ACKNOWLEDGEMENT
This work was supported by the Projects APVV-0677-11 and APVV-0029-16 of the Slovak Research and Development Agency and Project VEGA 2/0100/15 of the Slovak Scientific Grant Agency.

References

1. X. Wang, S. Xu, S. Zhou, W. Xu, M. Leary, P. Choong, M. Qian, M. Brandt, M. Xie, *Biomaterials*, 83 (2016) 127.

2. B. Wegener, B. Sievers, S. Utzschneider, P. Müller, V. Jansson, S. Rößler, P. Quadbeck, *Mater. Sci. Eng. B, 176 (2011)* 1789.
3. M. Moravej, D. Mantovani, *Int. J. Mol. Sci*., (2011) 4250.
4. G. Song, S. Song, *Adv. Eng. Mater*., 9 (2007) 298.
5. M. Peuster, C. Hesse, T. Schloo, Ch. Fink, P. Beerbaum, Ch. Schnakenburg, *Biomaterialia,* 27 (2006) 4955.
6. M. Schinhammer, I. Gerber, A.C. Hanzi, P.J. Uggowitzer *Mater. Sci. Eng .C,* 33 (2013) 782.
7. B. Liu, Y. F. Zheng, *Acta biomater.*,3 (2011) 1407.
8. M. Moravej, F. Prima, M. Fiset, D. Mantovani, *Acta biomater.* 6 (2010) 1726.
9. S. Zhu, N. Huang, L. Xu, Y. Zhang, H. Liu, Y. Lei, H. Sun, Y. Yao, *Surf. Coat. Tech*., 203 (2009) 1523.
10. A. Purnama, H. Hermawan, J Couet, D. Mantovani, *Acta biomater*., 6 (2010) 1800.
11. M. Schinhammer, A.C. Hänzi, J.F. Löffler, P.J. Uggowitzer, *Acta biomater*., 31 (2010) 1705.
12. H. Hermawan, H. Alamdari, D. Mantovani, D. Dube, *Powder. Metall., 51* (2008) 38.
13. J. Levesque, H. Hermawan, D. Dube, D. Mantovani, Design, *Acta Biomater*., 4 (2008) 284.
14. F. Witte, V. Kaese, H. Haferkamp, E. Switzer, A.M. Linderberg, C.J. Wirth, H. Windhagen, *Biomaterials,* 26 (2005) 3557.
15. F. Witte, J. Fischer, J. Nellesen, H.A. Crostack, H. V. Kaese, A. Pisch, H. Windhagen, *Biomaterials,* 27 (2006) 1013.
16. L. D. Zardiackas, D. E. Parsell, L. D. Dillon, D.W. Mitchell, L.A. Nunnery, R. Poggie, *J. Biomed. Mater. Res.,* 58 (2001) 180.
17. A. J. T. Clemow, A. M Weinstein, J .J Klawitter, J. Koeneman, *J. Biomed. Mater. Res.* 15 (1981) 73.
18. Alavi, R., Trenggono, A., Champagne, S. H. Hermawan, *Metals,* 7 (2017), 202.
19. A.Oriňak, R. Oriňaková, Z.O. Králová, A. Turoňová, M. Kupková, M. Hrubovčáková, R. Džunda, *J.Porous Mat.,* 21 (2014) 131.
20. R. Oriňaková, A. Oriňak, L. Bučková, M. Giretová, M. Medvecký, Ľ. Labbanczová, M. Kupková, M. Hrubovčáková,K. Kovaľ, *Int. J. Electrochemi. Sci.,* 8 (2013) 12451.
21. Z. Wen, L. Zhang, C. Chen, Y. Liu, C. Wu, C. Dai, *Mater. Sci. Eng. C,* 33 (2013) 1022.
22. A.H.M. Yusop, N.M. Daud, H. Nur, M.R.A. Kadir, H. Hermawan, *Sci. Rep., UK* 5 *(2015)* Article No. 11194
23. N.M. Daud, N.B. Sing, A.H. Yusop, F.A.A. Majid, H. Hermawan, *J. Orthop. Translation*, 2 (2014) 177.
24. J. He, F L. He, D.W. Li, Y.L. Liu, D.C. Yin, *Colloid. Surface B,* 142 (2016) 325.
25. M. Hrubovčáková, M. Kupková, M. Džupon. *Adv. Mat. Sci. Eng*. (2016) http://dx.doi.org/10.1155/2016/6257368.
26. U. Schwertmann, *Plant Sol.,* 130 (1991) 3.
27. S.O. Lee, T. Tran, B.H. Jung, S.J. Kim, M.J. Kim, *Hydrometall.,* 87 (2007) 91.
28. V.N. Malheiro, R.L. Spear, R.A. Brooks, A.E. Markaki, *Biomaterials*, 32 (2011) 6883.
29. J. Li, Y. Song, S. Zhang, C. Zhao, F. Zhang, X. Zhang, *Biomaterials*, 31 (2010) 5782.
30. S. Wang, D.H Kempen, M.J. Yaszemski, L. Lu, *Biomaterials*, 30 (2009) 3359.
31. M.P. Staiger, A.M. Pietak, J. Huadmai, G. Dias, *Biomaterials*, 27 (2006) 1728.
32. J. Li, Y. Song, S. Zhang, C. Zhao, F. Zhang, X. Zhang, L. Cao, Q. Fan, T. Tang, *Biomaterials*, 31 (2010), 5782.
33. A. Costan, N. Forna, A. Dima, M. Andronache, C. Roman, V. Manole, L. Stratulat, M. Agop,
J. Optoelectron. *Adv. Mater*., 3 (2011) 1338.
34. M.F. Ulum, A. Arafat, D. Noviana, A.H. Yusop, A.K. Nasution, M.R. Abdul Kadir, H. Hermawan, *Mater. Sci. Eng. C* 36 (2014) 336.
35. K.Y. Renkema, R.T. Alexander, R.J. Bindels, J.G. Hoenderop, *Ann. Med*., 40 (2008) 82.
36. J.H. Jo, Y. Li, S.M. Kim, H.E. Kim, Y.H. Koh, *J. Biomater. Appl.,* 28 (2013) 617.

37. K. Rezwan, Q.Z. Chen, J.J. Blaker, A.R. Boccaccini, *Biomaterials*, 27 (2006) 3413.
38. M. Yazdimamaghani, M. Razavi, D. Vashaee, L. Tayebi, *Mater. Lett.* 132 (2014) 106.
39. Y. Ramot, M. Haim-Zada, A.J, Domb, A. Nyska. *Adv. Drug Deliver. Rev.* 107 (2016) 153.
40. Ľ. Medvecký, R. Štulajterová, *Powder Metall. Progress* 8 (2008) 35.
41. X. Wang, S. Xu, S. Zhou, W. Xu, M. Leary, P. Choong, M. Qian, M. Brandt, M. Xie, *Biomaterials*, 83 (2016) 127.
42. C.E. Wen, M. Mabuchi, Y. Yamada, K. Shimojima, Y. Chino, T. Asahina, *Scripta Mater.*, 45 (2001) 1147.
43. Kennedy, *Powder Metallurgy*, 2012, *InTECH Open Access Publisher*, www.interchopen.com.
44. Stipniece, I. Narkevica, M. Sokolova, J.Locs, J. Ozolins, *Ceram. Int.* 42 (2016) 1530.
45. E. Alsberg, H.J. Kong, Y. Hirano, MK Smith, A. Albeinruti, D.J. Mooney, *J. Dent. Res.,*82 (2003) 903.
46. Wang, Y. Zheng, J. Liu, C. Jiang, Y Li, *Mater. Sci. Eng. C*, 71 (2017) 60.
47. S. Farah, D.G. Anderson, R. Langer,. *Adv. Drug. Deliver. Rev.,* 107 (2016) 367.
48. R. Oriňaková, A. Oriňak, M. Kupková, M. Hrubovčáková, L. Markušová-Bučková, M. Giretová, Ľ. Medvecký, E. Dobročka, O. Petruš, F. Kal'avský, *Int. J. Electrochem. Sci.*, 10 (2015) 8158.
49. L. Xu, E. Zhang, K. Yang, *J Mater Sci Mater Med.*, *20* (2009) 859.
50. H. Dieringa, L.Fuskova, D. Fechner, C. Blawert, Proceedings of ICCM17 Edinburgh, 27-31 July 2009, Edinburgh, UK (B1:9).
51. M. F. Ashby, L. Gibson, A. Evans, *Metal Foams,* 2000 Butterworth-Hainemann, Oxford, UK.
52. J. Teo, S.C. Wang, S.H. Teoh, *Spine*, 32 (2007) 1320.
53. C.V. Rahman, G. Kuhn, L.J. White, G.T. Kirby, O.P Varghese, J.S.McLaren. K.M. Shakesheff, *J. Biomed. Mater. Res. B,* 101 (2013) 648.
54. S. Novak, J. Druce, Q.Z. Chen, A.R. Boccaccini, *J. Mater. Sci.*, 44 (2009), 1442.
55. Y. Wang, L. Liu, S. Guo, *Polym. Degrad. Stabil.*, 95 (2010), 207.
56. T. Li, J. Lee, T. Kobayashi, H. Aoki, *J. Mat. Sci. Mater. M.*, 7 (1996), 355.
57. G.Daculsi, E. Goyenvalle, R. Cognet, E Aguado, E.O. Suokas, *Biomaterials*, 32 (2011) 3166.
58. X. Lu, Y.Leng, Q.Y. Zhang, *Surf. Coat. Technol*., 202 (2008) 3142.